

Multi-Objective Optimization of Flexible Pavement Design from an Environmental and Economic Perspective

Abrohom Demir

7 October 2022

Abstract

In recent years, construction companies have been pressured by clients to deliver infrastructure that are not only affordable but also environmental-friendlier. One of these infrastructures are flexible road pavements that are multi-layered systems where each layer can have its own type of mixture and thickness. The current number of asphalt mixtures available to contractors is increasing in size, creating an enormous number of flexible pavement design alternatives. The increasing size of the asphalt mixture portfolio makes it difficult for the pavement designer to find simultaneously the most affordable and environmental-friendly design, while ensuring that pavement performance requirements are met. In this thesis a constrained multi-objective optimization (CMOO) approach which uses the weighted sum method and genetic algorithm (GA) is developed to find optimal pavement designs by minimizing the Environmental Costs Indicator (ECI) and construction costs. The CMOO approach was applied to several case studies and shows that it can find optimal solutions for each case. Additionally, the CMOO approach enables the reduction of both ECI and construction costs when comparing the optimal pavement design with the original one made by the pavement designer. Finally, it is recommended that design responsibility of flexible pavements should be handed over from client to contractor in order to prevent the design of pavement structures that result in unnecessary additional environmental impacts and costs.

1. Introduction

It is no secret that a well-connected road network plays an important role in improving the economy of a country. Such a road network allows for the efficient transportation of goods, people and services. Consequently, the local, regional and national governmental bodies are willing to invest large sums of financial resources in their road network to ensure that their respective economies will improve. Since road networks predominantly consist of flexible pavements, these types of asphalt-paved surfaces can be considered as the main culprit with respect to road network costs.

In addition to the large cost involved, the construction of flexible pavements is also an environmentally damaging process (Espinoza et al., 2019). As a result, clients are increasingly pressuring contractors to minimize both costs and environmental impacts during the production, transportation and construction stages of flexible pavements, while demanding that pavement performance requirements are met. That has led bid assessments to deviate from the traditional cost-based approach to a new approach in which environmental aspects are also included in the set of bidding criteria (Garbarino et al., 2016).

A promising way of enabling the design of both cheaper and more environmentally friendly flexible pavement structures consists of optimizing the pavement design process. Flexible pavement structures are multi-layered systems consisting of up to seven layers, where the design considers the type of mixtures and thickness assigned to each layer as variables. Depending on the number of mixtures the contractor has in its portfolio, the number of alternative designs can become large making it difficult for a human decision-maker (DM) to find the most environmentally friendly and cheapest pavement structures that are still able to meet pavement performance requirements.

Usually, pavement performance requirements relate to both bottom-up fatigue cracking caused by the horizontal tensile strain at the bottom of the asphalt layers and permanent deformation caused by a vertical compressive strain on top of the subgrade layer (Strickland, 2015). These two strains are the critical strains determining the performance of the pavement structure. Traditional flexible pavement design methods as described in *The Bitumen Shell Handbook* (Strickland, 2015; Vasudevan et al., 2015) and Huang (2004), are commonly used to ensure that critical strain values are not exceeded. These methods are an iterative and trial-and-error based way of determining the structure of a flexible pavement that satisfy these pavement performance requirements without an integrated approach that simultaneously accounts for costs and environmental impacts. In doing so, a sub-optimal design is frequently selected over a cheaper and more environmentally friendly design.

Optimization studies have assessed the effect of layer resilient moduli and thicknesses on pavement performance (Peddinti et al., 2020; Saride et al., 2019). By considering a four-layered flexible pavement system, the reliability of the design based on rutting and fatigue failure was optimized by varying layer moduli and thicknesses. An analysis was made on which layer properties were deemed to influence pavement performance reliability significantly. Sahis & Biswas (2021) considered a three-layered flexible pavement system and attempted to optimize the thickness of both the bituminous and unbound subbase layer in order to improve pavement performance. This was done using Boussinesq's theory and Odemark's method (Odemark, 1949) to determine the critical strains and transform the three-layered system into a homogenous system, respectively.

In addition to the exclusive consideration of pavement performance in optimization-based pavement design approaches, the scientific community has steadily adopted a more integrated approach in which cost models are the basis for objective functions to be minimized. Rajbongshi & Das (2008) adopted such an approach with the objective of minimizing costs while meeting pavement performance reliability requirements. The development of cost-effective design charts depicting optimal layer thicknesses was proved to be an improved methodology when compared to traditional flexible pavement design methods. Dilip & Babu (2021) developed a reliability-based design optimization approach to determine optimal layer thicknesses that lead to the lowest costs while maintaining acceptable pavement reliability levels with respect to fatigue and rutting. Gaurav et al. (2011) integrated a costs-based model with pavement performance constraints based on the Mechanistic-Empirical Pavement Design Guide (MEPDG) which led to optimized layer thicknesses. Additional optimization studies were performed for minimizing costs and meeting design criteria for rigid (Hadi & Arfiadi, 2001) and flexible pavement design (Pryke et al., 2006). Both studies showing that construction costs can be reduced while pavement performance criteria are still met.

From the literature described above, it is clear that the current state of the optimization-based flexible pavement design approach focuses only on costs and pavement performance. Such an approach is ill-prepared to accommodate the new and pressing needs of contractors who see in the minimization of the environmental impacts of their flexible pavement construction projects an opportunity to leapfrog directly to a greener construction sector. Despite such developments, no optimization study has yet attempted to fill this gap in knowledge. Hence, a constrained multi-objective optimization (CMOO) approach applied to the design of flexible pavements is needed which considers the concomitant minimization of construction costs and environmental impacts while ensuring that pavement performance requirements are met. Such an approach should do so by enabling the selection of mixtures and thicknesses used in each layer in order to find the globally optimal pavement design for any given traffic volume.

With that being said, the research objectives of this work are twofold: (1) to develop a CMOO approach for the design of flexible pavement considering costs, environmental impact indicators and pavement performance requirements, using as example the Dutch context and (2) propose optimal flexible pavement structures that meet performance requirements at the lowest construction costs and environmental impacts scores for different traffic volumes.

To achieve these objectives the following outline is used in the paper. Section 2 presents the model formulations to be used by the solution method. These consists of describing the mathematical formulations of the objective functions and constraints. Section 3 elaborates on the solution method utilized to solve the CMOO problem. Section 4 presents the case studies used to illustrate the applicability of the proposed approach. Section 5 details the results of the application of the CMOO approach to the case studies which are discussed in Section 6. Finally, Section 7 provides concluding remarks on the main advancements presented in this paper.

2. Constrained multi objective optimization (CMOO) model formulation

The proposed CMOO approach for the flexible pavement design problem described in this paper consists of several models and components that can be used to calculate the objective functions values and constraints. Its architecture is illustrated in Figure 1, whereas further details on the several models and components is presented in the upcoming sub-sections.

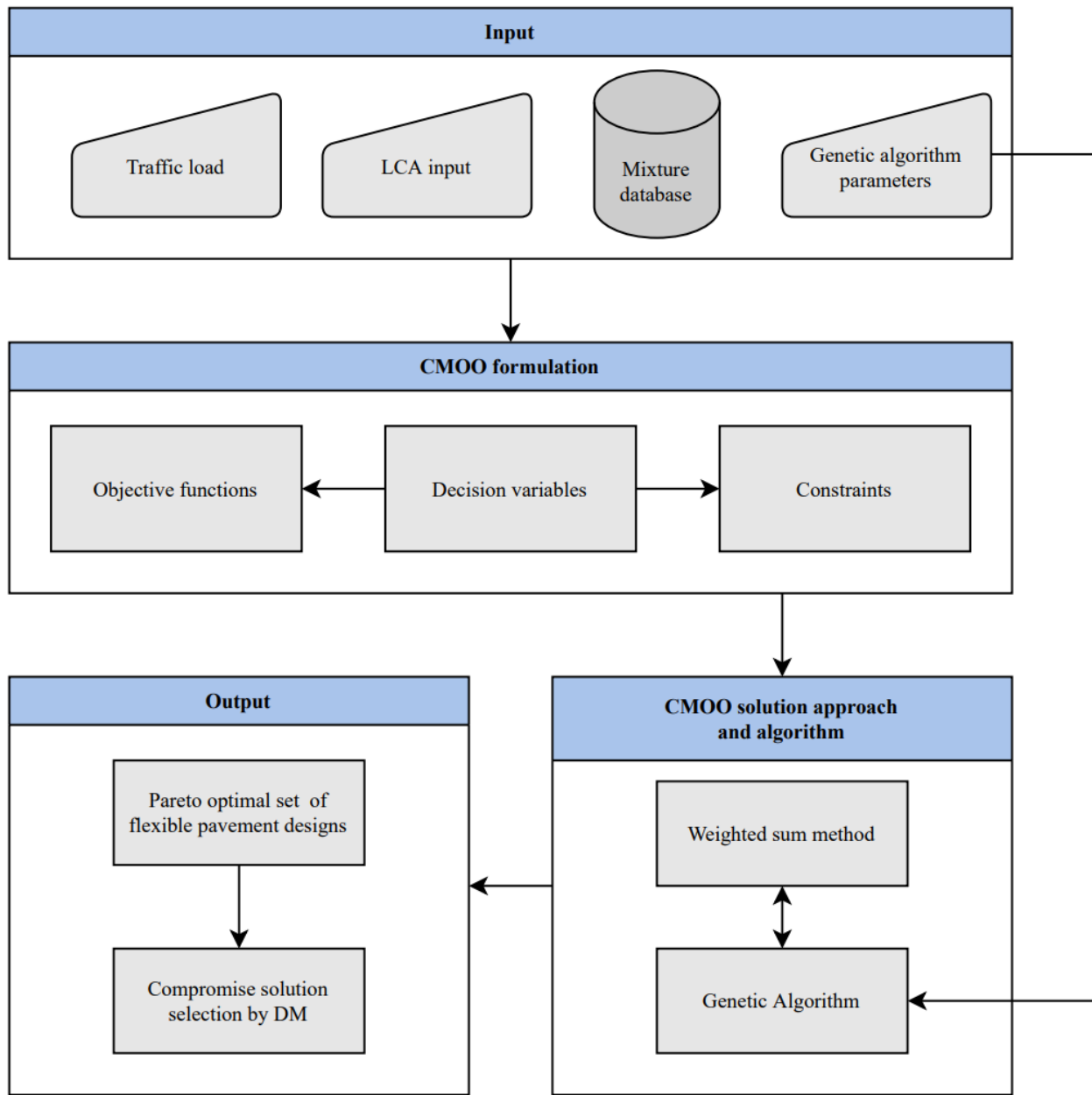


Figure 1. Architecture of the CMOO approach for the flexible pavement design problem

2.1. Nomenclature

The abbreviations used for outlining the model formulation and respective definition can be found in Table 1.

Table 1. Nomenclature adopted in the formulation of the CMOO approach for the flexible pavement design problem

Abbreviation	Definition (unit)	Abbreviation	Definition (unit)
Objective functions			
ECI	Environmental Costs Indicator of the pavement designs (<i>euro/m²</i>)	C	Construction costs of the pavement designs (<i>euro/m²</i>)
ECI_i^{A1-3}	The ECI for LCA stages A1, A2 and A3 for the mixture used in layer i (<i>euro/ton</i>)	C_i^{A1-3}	Costs of LCA stages A1, A2 and A3 for the mixture used in layer i (<i>euro/ton</i>)
ECI^{A4}	The ECI for LCA stage A4 (<i>euro/tkm</i>). Linearly deduced from Bak et al. (2022)	C^{A4}	Costs of LCA stage A4 (<i>euro/tkm</i>)
ECI_i^{A5}	The ECI for LCA stage A5 for the mixture used in layer i according to Bak et al. (2022) (<i>euro/ton</i>)	C^{A5}	Costs of LCA stage A5 (<i>euro/day</i>)
L	Number of layers in the pavement structure, where the maximum value is equal to 7 (-)	i	Layer number with $i = 1$ being the surface layer and $i = 7$ being the subbase layer (-)
h_i	Thickness of layer i (m)	ρ_i	In-situ density of layer i (<i>tonnes/m³</i>)
D_i	Transportation distance from the plant where the mixture used in layer i is produced to the project location (km)	R_i	Construction rate for the mixture used in layer i according to Bak et al. (2022) (<i>tonnes/day</i>)
Constraints			
TI	Truck intensity in one direction (<i>trucks/day</i>)	v	Vehicle speed (<i>km/h</i>)
PC_{road}	The performance class of the road based on the TI and v (-)	PC_i	The performance class of the mixture in layer i (-)
$h_i^{(L)}$	Lower boundary thickness value of the mixture in layer i (m)	$h_i^{(U)}$	Upper boundary thickness value of the mixture in layer i (m)
M_f^f	Miner's number for fatigue failure that is calculated (-)	M_f^r	Miner's number for rutting failure that is calculated (-)
M_f^a	Allowable Miner's number for fatigue failure (-)	$M_f^r^a$	Allowable Miner's number for rutting failure (-)
n_{ij}^f	Number of design load repetitions for fatigue failure for axle load category l and tire configuration j (-)	n_{ij}^r	Number of design load repetitions for rutting failure for axle load category l and tire configuration j (-)
N_{ij}^f	Allowable number of design load repetitions to prevent fatigue failure for axle load category l and tire configuration j (-)	N_{ij}^r	Allowable number of design load repetitions to prevent rutting failure for axle load category l and tire configuration j (-)
SDB_j^f	Relaxation factor for scattered driving behaviour i.e., not all traffic drives over the same spot, for fatigue failure for tire configuration j (-)	SDB_j^r	Relaxation factor for scattered driving behaviour i.e., not all traffic drives over the same spot, for rutting failure for tire configuration j (-)
ε_{ij}^t	Horizontal tensile strain at the bottom of the asphalt structure for axle load category l and tire configuration j ($\mu m/m$)	ε_{ij}^c	Vertical compressive strain at the top of the subgrade layer for axle load category l and tire configuration j ($\mu m/m$)
D_f	Allowable damage factor given by the client to determine M_f^a (-)	H_f	Healing factor against fatigue failure (-)
E_a	Equivalent stiffness of the entire asphalt structure (MPa). It depends on stiffness parameters of each mixture (see Appendix A)		
AL	Number of axle load categories, where the maximum value is equal to ten (-)	l	Axle load category (-)
TC	Number of tire configurations, where the maximum value is equal to four (-)	j	Tire configuration category (-)
P_l	Contribution of axle load category l to N_d (%)	P_j	Contribution of tire configuration j to N_d (%)
N_d	Total number of design load repetitions (-)	ADT	Average daily traffic (<i>veh/day</i>)
T	Percentage of trucks in the ADT (%)	a_{axle}	Average number of axles on a single truck (-)
W	Number of working days that the road is active (<i>days</i>)	Dir_f	Directional distribution factor of truck traffic (-)
L_f	Lane distribution factor of truck traffic (-)	G_f	Growth factor of truck traffic over the entire design life of the road (-)
t	Design life of the flexible pavement design (<i>years</i>)	v_f	Correction factor for traffic speed (-)
U	Correction factor for uncertainty in counting data (-)		

2.2. Decision variables

The flexible pavement design can be changed by varying the thickness and mixture of each layer. In the Netherlands, the design of a flexible pavement can consist of up to six asphalt layers, and usually one subbase layer is added in between the subgrade layer and the asphalt structure (Bouman et al., 2012). The natural subgrade layer is fixed and therefore is not considered a decision variable. Since each of the seven layers can have both a thickness and

mixture assigned to it, the decision vector \vec{X} consists of 14 decision variables each being represented as a real number. In mathematical language, $\vec{X} \subset \mathbb{R}^n$ with n being equal to 14.

2.3. Objective functions

The two objective functions that will be minimized in the CMOO approach are the cradle-to-laydown environmental impacts and corresponding costs of the Dutch flexible pavement construction process. The mathematical formulation is elaborated upon in this section.

2.3.1. Minimization of the environmental cost indicator (ECI)

The environmental impact minimization is based on the Environmental Costs Indicator (ECI) methodology described by de Bruyn et al. (2017). The ECI expresses all environmental impacts as one single value in euro per ton. More specifically, it corresponds to the costs of preventive measures for the government to avoid these environmental impacts. The ECI methodology can be seen as a weighting methodology of the impact assessment stage of a typical Life Cycle Assessment (LCA) study. The weighting factors used in the Netherlands are the so-called ECI weights, which are based on the shadow price methodology. The system boundaries of the LCA study underlying to the calculation of the present objective function only comprise the phases A1-A5 (Figure 2).

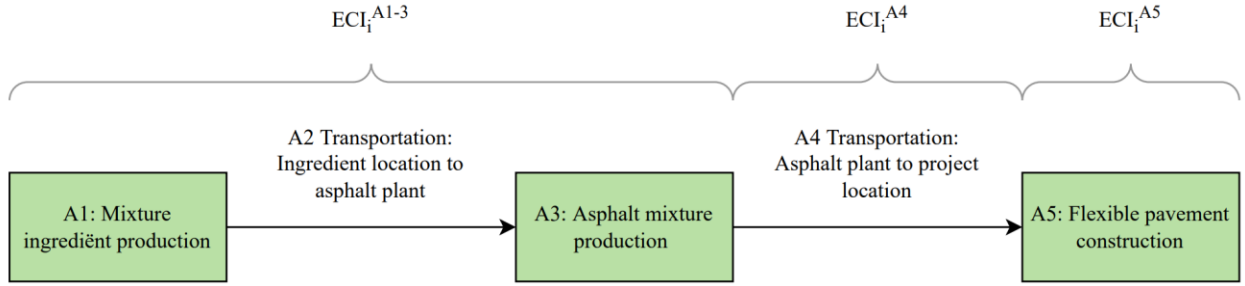


Figure 2. System boundaries of the LCA considered in the CMOO approach for the flexible pavement design problem

The Dutch asphalt sector incorporates the ECI methodology in the Product Category Rules for asphalt mixtures also known as NL-PCR Asphalt 2.0 (Van der Kruk & Overmars, 2022). This report contains the methodology which explains how ECIs are calculated for asphalt mixtures by using Environmental Product Declarations (EPDs) within the Ecochain software (Ecochain Helix, 2022). The ECI related to the production stages (i.e., A1-A3) are retrieved using the Ecochain software. In turn, the ECI related to the transportation and construction stages, (i.e., A4 and A5, respectively) are retrieved from Bak et al. (2022), which shows average ECI values for the different LCA stages per mixture in the Dutch asphalt sector by using a fictitious asphalt plant and pavement project location. These ECI values are used by default by contractors when specific A4 or A5 ECI values not available, which also is the case in the CMOO problem described in this paper. The ECI objective function is mathematically expressed in Eq. 1.

$$\text{Minimize ECI} = \sum_{i=1}^L h_i \times \rho_i (ECI_i^{A1-3} + ECI_i^{A4} \times D_i + ECI_i^{A5}) \quad (1)$$

2.3.2. Minimization of construction costs

Similarly, the cost minimization of the construction process of flexible pavements is also based on the production, transportation and construction stages, i.e. A1 until A5 (Figure 2). The construction rate per mixture (*tonnes/day*) for the cost calculation of stage A5 is retrieved from Bak et al. (2022). The cost objective function is mathematically expressed in Eq. 2.

$$\text{Minimize } C = \sum_{i=1}^L h_i \times \rho_i (C_i^{A1-3} + C^{A4} \times D_i + C^{A5} \times R_i) \quad (2)$$

2.4. Constraints

The Dutch context for the design of flexible pavements follows the guidelines proposed by Bouman et al. (2012), which are meant to help the pavement designer in designing flexible pavements that can cope with common flexible pavement failure mechanisms. The optimization constraints in the proposed methodology are in accordance with these guidelines unless specifically mentioned otherwise. There are three constraints which will be discussed in this section: (1) decision variable constraints, (2) the constraint related to bottom-up fatigue cracking, and (3) the constraint related to rutting.

2.4.1. Decision variable constraints

The Dutch asphalt sector considers four standard traffic classes (Standaard RAW Bepalingen, 2020) based on the daily truck intensity (TI) and the traffic speed (v), which are presented in Table 2. Each traffic class represents the so-called performance class of the road (PC_{road}) (Eq. 3). Asphalt mixtures are also assigned performance classes (PC_i) indicating whether they can be used in a given pavement structure. The complete dataset of all mixtures and their PCs considered in the case studies used to illustrate the proposed CMOO approach presented in this paper are shown in Appendix A.

$$PC_{road} \in \{PC_1, \dots, PC_4\} \quad (3)$$

The order in which layers are presented are important for the validity of the design of flexible pavement structures. Typically, flexible pavement structures consist of at least a surface, base and subbase layer, in that order. The compulsory layers, their order and required data are shown in Table 3.

Finally, each mixture is allowed to have a certain thickness ranging between a lower and upper boundary based on Specificaties Ontwerp Asfaltverhardingen (2016), henceforth referred to as SOA. The dataset in Appendix A shows these boundaries which are mathematically described in Eq. 4.

$$h_i^{(L)} \leq h_i \leq h_i^{(U)}, \forall i \in L \quad (4)$$

Table 2. Dutch traffic classes

Truck intensity (TI) (trucks/day)	Traffic speed (v) (km/h)	PC_{road}
$TI < 50$	$v > 15$	1
$50 \leq TI \leq 2500$	$v > 15$	2
$TI > 2500$	$v > 15$	3
$TI > 250$	$v \leq 15$	4

Table 3. Layer order and required data for constraint calculations

Layer no.	Layer type	Compulsory	Thickness	Stiffness parameters	Fatigue parameters	Poisson's ratio
1	Surface	X	X	X		X
2	Bind		X	X		X
3	Base		X	X		X
4	Base		X	X		X
5	Base		X	X		X
6	Base	X	X	X	X	X
7	Subbase	X	X	X ¹		X
8 ²	Subgrade (sand)	X		X ¹		X

¹ For subbase and subgrade stiffnesses, a single value is assumed in MPa. No stiffness calculation based on parameters is needed.

² Subgrade layer type and thickness are not considered as decision variable since they are always present and pre-established in practice. Thickness of the subgrade is fixed as it is always assumed to be infinite.

2.4.2. The bottom-up fatigue cracking failure constraint

The pavement structure in the optimization approach is subject to a range of different axle loads and tire configurations (ALTC), that amounts to 40. The damage contribution of each combination to the pavement performance can be calculated and combined with all the other configurations using Miner's law (Miner, 1945).

For bottom-up fatigue cracking the horizontal tensile strain at the bottom of the asphalt pavement structure needs to be calculated for every ALTC. For this purpose, the Adaptive Layered Viscoelastic Analysis (ALVA) model is used (Skar & Andersen, 2020). The ALVA model allows the calculation of the pavement response at any given point within the pavement, making it suitable for the optimization of the design of flexible pavement structures.

Miner's law in the context of bottom-up fatigue cracking failure and how it relates to the tensile strain at the bottom of the asphalt structure is mathematically expressed in Eq. 5-10. For definitions and units of each parameter, the reader is referred to Section 2.1.

$$M_f^c \leq M_f^a \quad (5)$$

$$M_f^a = \frac{1}{0.75 \times 10^{0.38 \times D_f}} \quad (6)$$

$$M_f^c = \sum_{l=1}^{AL} \sum_{j=1}^{TC} \frac{n_{lj}^f}{N_{lj}^f}, \forall l \in AL, \forall j \in TC \quad (7)$$

$$n_{lj}^f = P_l \times P_j \times N_d \times SDB_j^f, \forall l \in AL, \forall j \in TC \quad (8)$$

$$N_{lj}^f = H_f \times \exp(c_1^f + c_5^f \times \{\ln[\varepsilon_{lj}^t] + c_2^f \times \ln^2[E_a] + c_3^f \times \ln[E_a] + c_4^f\}^2), \forall l \in AL, \forall j \in TC \quad (9)$$

$$N_d = ADT \times T \times a_{axle} \times W \times Dir_f \times L_f \times G_f \times t \times v_f \times U \quad (10)$$

2.4.3. The rutting failure constraint

Similarly, the rutting constraint is also calculated using Miner's law. Instead of the horizontal tensile strain at the bottom of the asphalt pavement structure, the rutting constraint requires the ALVA model to calculate the vertical compressive strain on top of the subgrade layer. The relation between Miner's law and the vertical compressive strain on top of the subgrade layer is mathematically expressed in Eq. 11-15.

$$M_r^c \leq M_r^a \quad (11)$$

$$M_r^a = 1 \quad (12)$$

$$M_r^c = \sum_{l=1}^{AL} \sum_{j=1}^{TC} \frac{n_{lj}^r}{N_{lj}^r}, \forall l \in AL, \forall j \in TC \quad (13)$$

$$n_{lj}^r = P_l \times P_j \times N_d \times SDB_j^r, \forall l \in AL, \forall j \in TC \quad (14)$$

$$N_{lj}^r = 10^{(17.289 - 4 \log(\varepsilon_{ij}^c))}, \forall l \in AL, \forall j \in TC \quad (15)$$

3. Solution method

3.1 The constrained multi objective optimization (CMOO) approach

Although the ECI and cost objective functions are expressed in the same unit, the simple addition of objectives to create a single objective optimization (SOO) problem is not correct. The reason being that both objectives are valued differently i.e., 1 EUR in construction costs is not equal to 1 EUR in ECI. Instead, an adequate MOO approach is needed that allows for the solution method to evaluate the fitness of potential solutions based on both objectives.

Since the client, will put a certain emphasis on both objectives, preference-based MOO approaches are suitable for the flexible pavement design problem. For this reason, the weighted sum method (WSM) is chosen, as it can account for preference information both before and after solving the flexible pavement design problem, making it an a priori as well as an a posteriori method (Miettinen, 2008, 2012). The a priori version can be used if the DM is sure about the weights to be assigned to the objective functions, whereas the a posteriori version determines firstly the Pareto Front (PF) by calculating firstly the objective functions scores over several weighting sets, after which the DM can analyse the trade-offs between objective functions scores by looking at the PF. In a nutshell, the WSM transforms the MOO problem into a SOO problem. The SOO translation by using the WSM is mathematically expressed in Eq. 16. Where K is the total number of objective functions, k is objective function in question, w_k is the weight applied to objective function k , f'_k is the normalized score of objective function k , \vec{X} is the decision variable vector and S is the feasible solution search space.

$$\begin{aligned} \text{Minimize: } & \sum_{k=1}^K w_k \times f'_k(\vec{X}) \\ \text{subject to: } & \vec{X} \in S \\ & w_k \geq 0, \quad k = 1, \dots, K, \quad \sum_{k=1}^K w_k = 1 \end{aligned} \quad (16)$$

The model formulation is computationally expensive, in particular the calculation of the critical strain values through the ALVA model. The computational load can be reduced by increasing the step size between the different weight sets. Therefore, the step size of 0.1 is chosen.

Since the different objective functions might be of different orders of magnitude it is necessary to normalize their scores (Deb, 2001a). By minimizing and maximizing each objective separately i.e., with an extreme weight set, the normalization boundaries (i.e., 0-1) can be obtained. The normalized score for each objective function can be obtained by using Eq. 17. Where f_k is the score of objective function k and, f_k^{min} and f_k^{max} are the absolute objective scores when minimizing and maximizing objective function k , respectively.

Finally, the formulation of the CMOO model was written in MATLAB® programming software (*Matlab R2021b*, 2021).

$$f'_k(\vec{X}) = \frac{f_k(\vec{X}) - f_k^{min}}{f_k^{max} - f_k^{min}} \quad (17)$$

3.2. Solution algorithm

Many real-life MOO problems consist of non-differentiable or discontinuous functions, making it very difficult for exact algorithms not to fall in local optima (Deb, 2001a; Sivanandam & Deepa, 2008). Additionally, other studies argue that these real-life problems are highly complex and difficult for exact algorithms to solve (Talbi, 2009; Yu & Gen, 2010). Consequently, the use of metaheuristic algorithms in such cases is favoured. Hence, for the CMOO flexible pavement design problem described in this paper metaheuristics will be applied.

Within the category of metaheuristics, a wide variety of optimization algorithms exist e.g., Genetic Algorithm (GA), Particle Swarm Optimization (PSO), Simulated Annealing (SA), to name a few. These are also called evolutionary algorithms (EA). The comparison between EA and their variants has proven to be difficult and a choice for one specific EA variant can never be fully justified (LaTorre et al., 2020). Since GA is particularly easy to use and has a broad applicability (Deb, 2001a), including in the pavement sector (Ferreira & Santos, 2012; Santos et al., 2016, 2017a, 2017b, 2018), the approach proposed in this paper GA will also be applied to solve the CMOO flexible pavement design problem. Its working mechanism is illustrated in Figure 3 and described in the upcoming sub-sections, whereas the adopted parameters are summarized in Table 4.

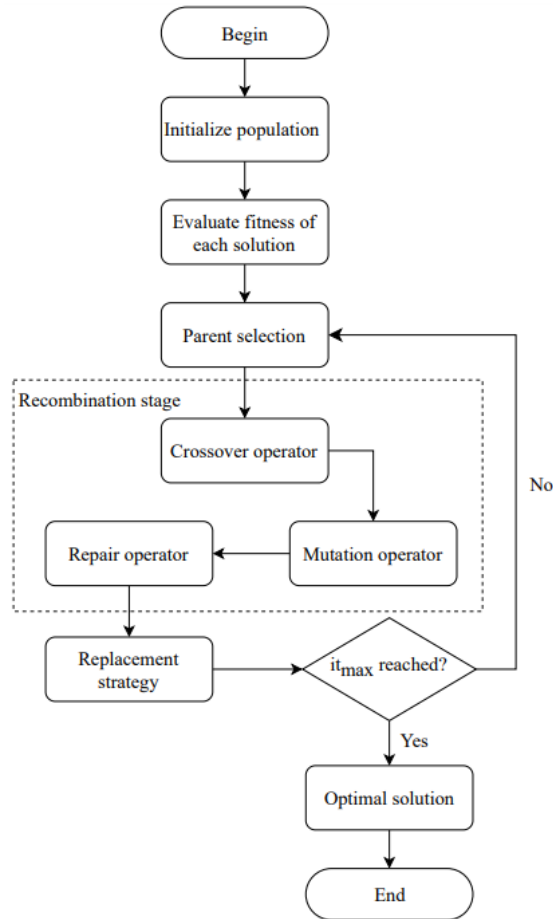


Figure 3. Working mechanism of GA

Table 4. Nomenclature adopted for GA parameters of the CMOO flexible pavement design problem

Abbreviation	Definition
N	Population size
CV	Constraint violation
\vec{X}	Decision variable vector, also known as the solution
z	Constraint number
Z	Total number of constraints
\bar{g}_z	The z^{th} normalized constraint violation
g_z	The z^{th} absolute constraint violation
g_z^{min}	Lowest z^{th} absolute constraint violation within the population
g_z^{max}	Highest z^{th} absolute constraint violation within the population
T_S	Tournament size for parent selection
P_c	Crossover probability
P_m	Mutation probability
T_R	Tournament size for the replacement strategy
p_e	Elitism preservation operator
it_{max}	Maximum number of iterations

3.2.1. Population initialization

GA implements a stochastic search procedure in order to find the global optimal solution. The first step is to initialize the population randomly based on the decision variable constraints. In doing so, a population with N solution individuals are created.

3.2.2. Selection method

The second step consists of selecting the parents to go through the recombination stage. The idea behind the selection step is to stimulate the reproduction of fitter parents with the objective of producing even fitter offspring. Tournament selection is chosen as the selection method because it is used in NSGA-II (Deb et al., 2002) which is a widely used GA variant. The steps of tournament selection are described below:

1. Calculate the weighted sum objective function value of each parent.
2. Calculate the constraint violation (CV) using Eq. 18 and 19.

$$CV(\vec{X}) = \sum_{z=1}^Z \bar{g}_z(\vec{X}) \quad (18)$$

$$\bar{g}_z(\vec{X}) = \frac{g_z(\vec{X}) - g_z^{min}}{g_z^{max} - g_z^{min}} \quad (19)$$

Where \vec{X} is the solution individual, \bar{g}_z is the z^{th} normalized CV. The normalized CV is calculated using a similar approach as described in Eq. 17, but here the normalization boundaries are considered to be those of the population (Deb, 2001b).

3. Create N tournaments with each tournament having size T_S for parent selection. An increase in T_S , results in higher selection pressure. Additionally, each tournament pool is randomly filled with T_S parents.
4. Determine the winners based on the same approach as proposed in NSGA-II. This includes defining three possible scenarios.
 - a. All tournament solutions are feasible solutions, and the winner is selected based on the lowest weighted sum value.
 - b. All tournament solutions are infeasible solutions and the solution with the lowest CV is the winner.

- c. Tournament solutions include both feasible and infeasible solutions. Only the feasible solutions can win and among them the solution with the lowest weighted sum value is the winner.
5. Produce parent sets of size two based on tournament winners, which will go through the recombination stage.

3.2.3. Offspring generation

During the recombination phase the two parents in each parent set will mate and produce offspring through crossover. Furthermore, the genes of offspring will be changed randomly through the mutation operator. Finally, a repair operator is applied to fix solutions that violate the decision variable constraints after the crossover and mutation operators have been applied. There are two parameters which influence optimization quality. These are the crossover probability (P_c) and mutation probability (P_m). Offspring generation will occur using the following procedure:

1. The two parents within a parent set will exchange genetic material using single point crossover (SPC). Whether or not crossover will take place between the two parents is based on the P_c . Either way, two offspring individuals are created. As a result, an offspring population of size N is created.
2. The created offspring solutions in step 1 will also be mutated based on the P_m . Because the decision vector consists only of real numbers and is non-binary, the mutated gene in question will be assigned a random value that meets the decision variable constraints.
3. The crossover and mutation operator can cause invalid solutions to occur (Talbi, 2009). Consequently, a repair operator is used to check for invalid solutions and repairs them afterwards.

For the crossover operator, two-point crossover (TPC) and uniform crossover (UC) were also tested but resulted in worse optimization quality than SPC. When the order matters in the decision variable vectors, these last two crossover operators are more likely to disrupt fitter chromosomes than to improve their fitness (Reeves, 2010; Sivanandam & Deepa, 2008)). Two SPC operators are applied simultaneously and independently on both the mixture type and thickness decision vectors. This way mixture type and thickness variables for a particular layer are not interlocked, which allows for more breathing room with the intention of finding a more diverse offspring population.

3.2.4. Replacement strategy

At this point there are two populations i.e., the parent and offspring populations, both of size N . Combining these two populations into one creates a population size of $2N$. Traditional GA maintain a fixed population size, meaning that not all parents and offspring can go to the next generation. For this purpose, a replacement strategy is needed that allows for fitter offspring solutions to replace worse parent solutions. The GA in the proposed approach incorporates a replacement strategy that includes a tournament for each spot in the next generation with tournament size T_R . Additionally, an elitism preserving operator (p_e) is included similarly to the NSGA-II approach. The idea is that during the replacement process $p_e N$ spots (rounded up) are reserved for the best solutions within that iteration. This way the best solution(s) across all iterations will never get lost. The remaining $N - p_e N$ spots will be filled using the tournament method discussed earlier. All the steps from Section 3.2.2. until 3.2.4 will be repeated for it_{max} iterations.

3.2.5. GA parameters calibration

Traditionally, GAs are computational expensive search algorithms whose quality of the “optimal” solutions depends on the parameter’s values adopted. By calibrating the GA parameters, a balance between computational time and optimization quality can be found. The best-found GA configuration for the CMOO flexible pavement design problem discussed in this paper is summarized in Table 5 and was obtained through a combinatorial trial-and-error approach.

Table 5. Algorithm parameters after calibration

N	T_s	P_c	P_m	T_R	p_e	it_{max}
200	2	0.95	1/14	16	0.01	40

4. Case studies

The developed CMOO approach is applied to a total of five case studies. Four cases are dedicated to the PCs shown in Table 2, whereas the fifth is a real-life case study for a municipal road in the city of Enschede, The Netherlands.

All case studies will use the same OIA and LCA input parameters which are shown in Table 6. The values of the OIA parameters are based on SOA which specifies what values to use if the client's quantification is not provided. The case studies are different from each other in terms of either the TI , v , plant-project distances or a combination of these. An overview of the differences between the characteristics of the case studies is given in Table 7. The dataset can be found in Appendix A. It is important to note that different construction costs and ECI (A1-3) values are used for the PC and the real-life case study. Due to confidentiality reasons, only the rankings of construction costs, ECI and material properties can be disclosed. Likewise, C^{A4} and C^{A5} values cannot not be disclosed due to the same reason. Noteworthy, the values for these last two input parameters are the same for all case studies.

Table 6. Value of the input parameters for all case studies

OIA input parameters	
Name	Value
Design period	20 years
Active days of road per year	270 days
Average axles per truck	3.5
Correction factor for directional distribution	1
Correction factor for lane distribution	1
Correction factor for uncertainty in counting data	1.75
Annual growth of traffic percentage	3.5 %
Lane width	3 m
Distance from tire to edge of road	0.25 m
Axle load range and distribution	Normal municipal road
Tire configuration distribution	Standard
Allowed damage percentage based on Miner's law	15 %
Confidence level	85 %
LCA input parameters	
Transportation ECI from plant to project	7.6×10^{-3} euro/tkm

Table 7. Case study characteristics

Case study ID	1	2	3	4	5
Case study type	PC 1	PC 2	PC 3	PC 4	Real-life
TI (trucks/day)	40	1225	3000	500	364
v (km/h)	50	50	50	10	50
Distance from plant 1 to project (km)	20	20	20	20	13.5
Distance from plant 2 to project (km)	100	100	100	100	94.9
Distance from plant 3 to project (for subbase mixtures) (km)	30	30	30	30	17.7

5. Results

This section presents the results of the application of the CMOO approach to the five case studies. They were obtained after running the optimization algorithm on a computational device featuring an Intel® Core™ i7-7700HQ CPU @2.80GHz, 2808 MHz, 4 Core(s), 8 Logical Processor(s), a NVIDIA® Quadro® M1200, 4GB VRAM and 16GB of RAM.

Table 8 presents the optimal decision variable vector and corresponding objective function and constraint values for each weighting set for case studies 1-4. The objective function values are depicted in the objective search space (Figure 4-7). The optimal solutions in Table 8 are determined using the GA configuration discussed in Section 3.2.5.

The iteration-wise improvement effect of the CMOO approach is depicted in Figure 9 which considers as example the generational improvement for ECI weight 0.6 and case study 3.

From the calculated Miner's numbers related to both fatigue and rutting failure it can be noted that fatigue failure is the most enforcing constraint, since the allowed Miner's numbers (M_f^a and M_r^a) according to Eq. 6 and 12 are equal to 0.54 and 1, respectively.

The results of the application of the CMOO approach to the real-life case study (case study ID number 5) are presented in Figure 8. This figure also includes the flexible pavement design defined by the pavement designer. Reductions in both objective function values were observed when applying the CMOO approach. These reductions are calculated in relation to the pavement design solution defined by the pavement designer and implemented in the project. The ECI objective function was reduced from 3.34 to 2.15 *euro/m²*, which corresponds to a reduction of 36%. The C objective function was reduced from 47.33 to 33.74 *euro/m²*, which corresponds to a reduction of 29%.

Table 8. Case study results showing the sets of optimal solution

ECI weights ¹	Case study ID	Optimal decision variable vector ^{2,3}	ECI (<i>euro/m²</i>)	C (<i>euro/m²</i>)	CV	M_f^c	M_r^c
0-1	1	{12,0,0,0,0,1,33,20,0,0,0,0,60,250}	1.49	30.59	0	0.5002	0.1272
0-0.6	2	{12,2,0,0,0,5,33,20,75,0,0,0,55,250}	2.21	42.45	0	0.5367	0.3420
0.7-0.8	2	{12,4,4,0,0,5,33,20,40,40,0,0,55,250}	2.19	43.07	0	0.4470	0.3052
0.9-1	2	{12,4,4,0,0,5,32,20,40,55,0,0,55,250}	2.17	44.51	0	0.5279	0.2500
0-0.7	3	{17,4,4,0,0,5,33,20,45,55,0,0,55,250}	2.37	46.50	0	0.4674	0.4419
0.8-1	3	{17,4,4,0,0,5,32,20,55,60,0,0,55,250}	2.35	47.94	0	0.5300	0.3595
0-1	4	{17,4,4,0,0,5,33,20,40,40,0,0,55,250}	2.19	43.29	0	0.5314	0.3027
0-0.6	5	{12,4,0,0,0,5,33,20,55,0,0,0,55,250}	2.15	33.74	0	0.4499	0.1936
0.7-1	5	{17,4,0,0,0,1,33,20,60,0,0,0,55,250}	2.14	34.18	0	0.5400	0.2078

¹ C weights can be obtained by subtracting the ECI weights from 1 as represented by Eq. 16.

² The vector should be read as the first and last seven elements representing the mixture and thickness applied to each layer. In essence, the vector comprises the mixture and thickness vectors, in this order, each having a size of seven where the first and last element for each one of these vectors represent the surface and subbase layer respectively.

³ Value of 0 indicates no layer is used in that position.

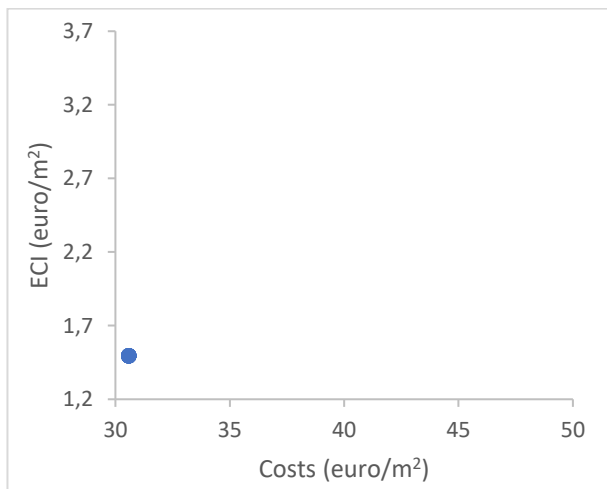


Figure 4. Optimal solution set of case study 1

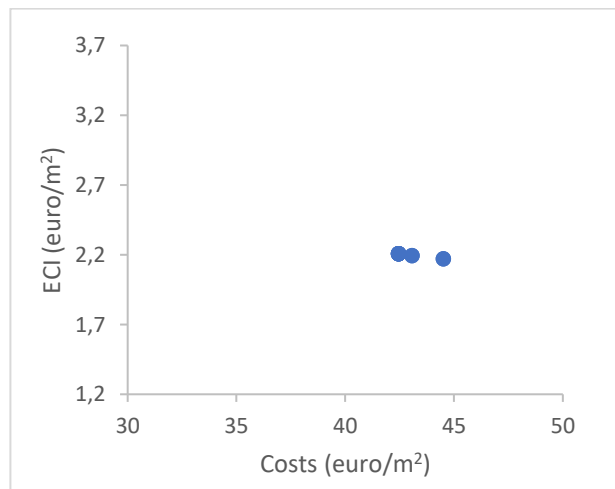


Figure 5. Optimal solution set of case study 2

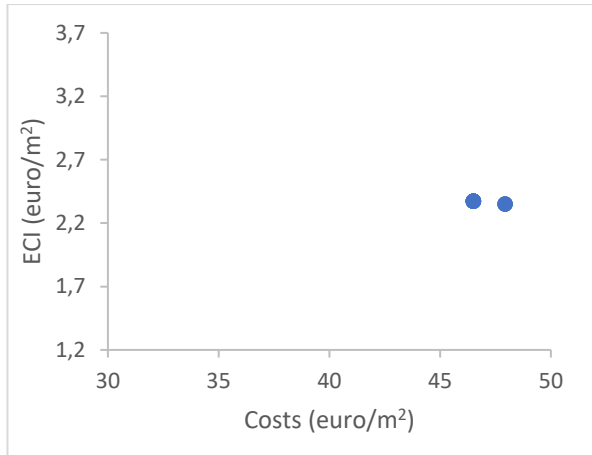


Figure 6. Optimal solution set of case study 3

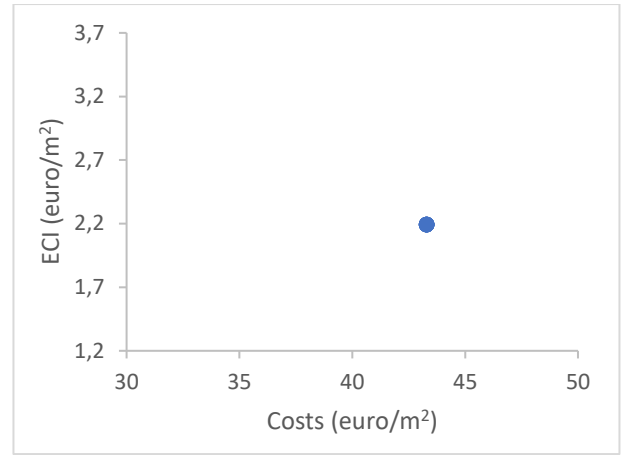


Figure 7. Optimal solution set of case study 4

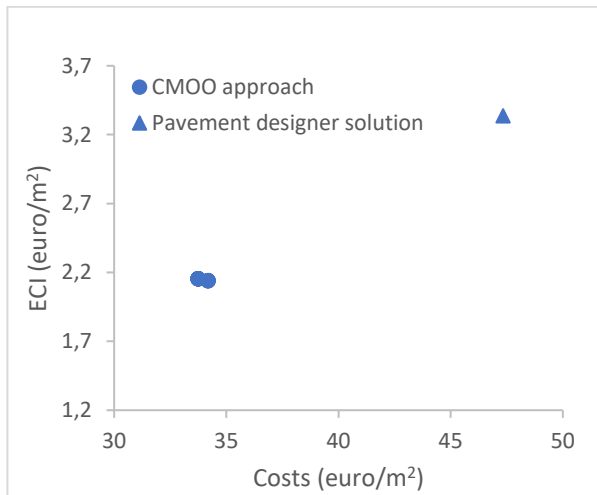


Figure 8. Optimal solution set of case study 5 compared to the pavement designer solution

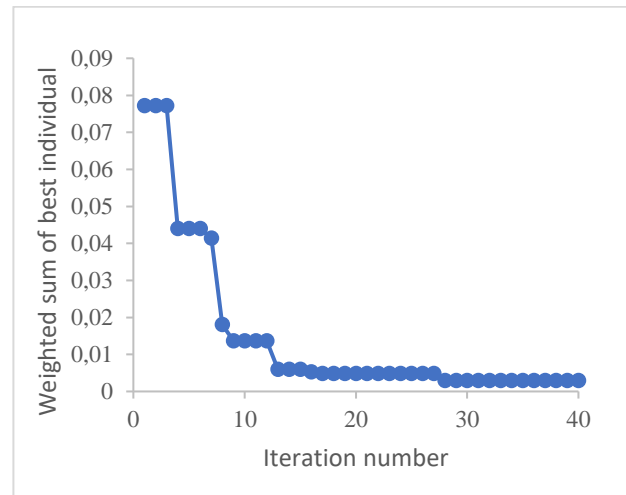


Figure 9. Iteration-wise improvement example from case study 3 and ECI weight 0.6

6. Discussions

6.1. Implications of optimal solutions

Three types of optimal solution sets were found for the different case studies. Solution sets with one optimal solution (case studies 1 and 4) indicate no trade-off possibilities and show that the same solution is optimal for both objective functions. Furthermore, two optimal solutions (case studies 3 and 5) indicate that all weighting sets lead to solutions that are optimal for one of the objective functions which are optimized individually. Case study 2 resulted in an optimal solution set with three optimal solutions. In this case the pavement designer can choose the optimal solution based on preference. The choice is between the cheapest, environmental-friendliest, or balanced solution.

Cases 1, 5, 2 and 3 have an increasing traffic volume which leads to the increase of the thickness of the total pavement structure. Note that case 4 also differs in traffic speed and therefore cannot be used to determine the relation between traffic volume and pavement structure thickness. However, when comparing cases 4 and 5 it becomes clear that a lower traffic speed with a similar traffic volume requires a thicker pavement structure.

Optimal solutions tend to be characterized by a dominant set of mixtures. Surface mixtures 12 and 17 are alternatively used in all optimal solutions. This can be explained by the fact that surface mixtures have higher costs and ECI values when compared to base/bind mixtures, meaning that the algorithm will favor designs with the thinnest surface layers. Within the current dataset the thinnest possible mixtures (20 mm) are 12 and 17-23 where the cheapest and the least environmentally burdensome mixture for PC1 and PC2 is 12 and for PC3 and PC4 is 17. Case study 5 is an exception where a different mixture-thickness combination outperforms this principle.

Additionally, the lowest-positioned base layer has the highest influence on total pavement thickness since bottom-up fatigue cracking is initiated in this layer and propagates upwards. The mixture with the best fatigue parameters is predominantly chosen for this layer i.e., mixture 5, with the minimum allowed thickness value (55 mm). Similarly to the surface mixtures, mixture 5 has a significantly higher ECI and cost values than the mixtures chosen in other base/bind layers. Therefore, the algorithm favors the lowest-positioned base layer to have the lowest possible thickness. Since the influence on total pavement thickness is high, it directly relates to the total ECI and costs of the pavement. This explains why one of the mixtures with the best fatigue characteristics is often chosen, despite being one of the most expensive base mixtures from the dataset. An exception to this is case study 1 and 5 where mixture 1 is selected above mixture 5. In these cases, the 5 mm that could be reduced from the total pavement thickness is not worth the additional costs and ECI of mixture 5 when comparing it to mixture 1.

Subbase mixture thickness of optimal solutions are also always set to the lowest possible thickness, but due to a different reason. ECI and cost values related to the production of subbase mixtures are the lowest, but they contribute the most to the mass of the pavement structure, and therefore have higher transportation and construction ECI and, more importantly, costs. For this reason, the algorithm favors designs with the thinnest possible subbase mixtures. When the weighting set favors ECI instead of costs, subbase mixture 32 is sometimes chosen. When the preferred weighting set is the opposite subbase mixture 33 is chosen.

Mixtures in layers between the most bottom base and surface layer get thicknesses defined in such a way that the design satisfies pavement performance criteria, whereas the previously mentioned mixtures i.e., surface, lowest-positioned base and subbase mixtures, always have a thickness equal to the lower thickness boundary. The most common mixtures selected by the CMOO approach are mixtures 2 and 4 depending on the required thickness for meeting pavement performance criteria. If the in-between layers require a combined thickness of 75 instead of 80 mm, this cannot be achieved with mixture 4. This is explained by the fact that the allowed thickness must be within 40-60 mm for one layer of mixture 4 and 55-90 mm for one layer of mixture 2. It is impossible to achieve the required 75 mm thickness with mixture 4 regardless of the use of one or two layers. However, it is possible to achieve this with one layer of mixture 2. Furthermore, in such cases the number of optimal solutions is higher than usual e.g., case study 2, meaning that the number of optimal solutions depends on mixture-thickness possibilities of a case.

Further, the optimal solutions and corresponding constraint values show that the CMOO approach is in line with Bouman et al. (2012), which states that for most cases fatigue failure will occur before rutting failure. This alignment with literature partly validates the constraint formulations in the CMOO approach.

Noteworthy is the difference in restrictions applied to the pavement designer and CMOO approach for case study 5. The pavement designer must adhere to requirements set by the client i.e., the flexible pavement design should contain a certain number of layers with thicknesses specified beforehand. Additionally, the number of applicable mixtures to be used per layer is also limited, thereby creating limited design freedom for the pavement designer. On the other hand, the CMOO approach assumes complete design freedom, allowing for cheaper and environmental-friendlier designs i.e., as shown by reductions of 29% and 36%, respectively (for an ECI weight of 0), when compared to the pavement designer approach.

Finally, pavement performance calculation requires the data on physical properties of mixtures to be known. Such data is only known by the asphalt plant owner and contractor. Notwithstanding the lack of data for pavement performance calculation, it is the client that prescribes the flexible pavement design. This confirms the inefficient approach characterizing the decision-making process in the Dutch asphalt sector identified by the literature (Bijleveld et al., 2015; Miller et al., 2010). Such an approach can lead to overdesigned road pavement structures and avoidable additional environmental impacts and construction costs as shown with case study 5.

6.2. Practical implications

From a practical point of view, the CMOO approach can be applied in a bidding procedure using the following steps. First, the input parameters including mixture dataset must be updated for the bid. Running the algorithm will result in one or several optimal solutions. The pavement designer can choose one of the optimal solutions based on his/her preference for environmental and economic aspects.

Secondly, the chosen solution must be tested again in the actual OIA software to ensure that no overdesign has occurred. The reason being that the optimal pavement structures defined by the CMOO approach are slightly thicker than the pavement structures obtained with the application of the OIA software. In the case of overdesign, the optimal pavement structure can be fine-tuned until the overdesign is overcome.

Finally, the optimal pavement structure should be sent to the contractor's calculation department to calculate the detailed ECI and costs of the pavement design. ECI and costs include very detailed components which are not included in the CMOO approach. To make the bid as detailed as required, the optimal pavement structure should be handed in to the contractor's calculation department which will make a detailed bid using the optimal solution.

6.3. Limitations of the CMOO approach

Obtaining the PF for a portfolio of 33 mixtures already is computationally expensive. If the dataset increases in size, the proposed GA parameter configuration would require recalibration. Both the recalibration process and new configuration itself will most likely require even higher computational times in order to maintain the optimization quality. A possible solution to decrease the computational time might be by pre-eliminating dominated mixtures from the dataset. Additional solutions for reducing the computational time can be found in the use of surrogate-based optimization (Gaurav et al., 2011) or Kriging metamodels (Dilip & Babu, 2021).

The calculation of pavement performance in the proposed CMOO approach does not consider the probabilistic nature of pavement design input parameters. Abed et al. (2019) argues that the variability of layer thickness and stiffness significantly impacts pavement performance. Therefore, ignoring uncertainties might result in under or overdesigned pavement structure by the CMOO approach.

The current model formulations always assume a fixed subgrade material type i.e., sand, where a subbase layer can be directly applied above the subgrade layer. In cases where the natural subgrade is a water-retaining material type, an additional sand layer is required between the subgrade and subbase layer. The current CMOO approach does not take this into account. Hence, only project locations where sand is the natural subgrade layer are suitable for the current version of the proposed CMOO approach.

Finally, the algorithm can only assume complete design freedom. That means that if the client establishes beforehand any thickness- or mixture-related requirements, the CMOO approach becomes inapplicable. This also includes cases where the client requires a specified number of layers in the design. Additionally, only projects concerning complete reconstruction are suitable for the CMOO approach.

7. Conclusions

The increasing number of possible flexible pavement design alternatives has made it difficult for pavement designers to find pavement designs that reduce both environmental impacts and construction costs while meeting pavement performance requirements. To solve this challenge, a CMOO approach has been developed that concomitantly minimizes environmental impacts and construction costs and uses GA to find optimal pavement design solutions from the different thickness-mixture combinations.

The proposed CMOO approach has been applied to five case studies. The results show that the approach is able to find optimal solution set for each case. Additionally, one of these case studies was based on a real-life project in which the original pavement design was compared with the optimal design found by the CMOO approach. The results show a significant reduction in both ECI and costs objective function values.

Since pavement designers have little design freedom due to heavy requirements set by the client, the CMOO approach shows that a change in the traditional approach of the asphalt paving sector can be very beneficial to all parties involved. This implies that design responsibility should be handed over from the client to the contractor, since the latter has access to mixtures data and therefore it is in a more favorable position to design pavement structures that are less environmentally harmful and economically onerous.

Acknowledgements

The author would like to thank TWW (Twentse Weg- en Waterbouw) and ReintenInfra for the opportunity given to carry out his MSc thesis and for sharing their facilities and data. Furthermore, the author would also like to thank Toni Messinella for the useful insights provided on the Dutch flexible pavement design procedure.

References

- Abed, A., Thom, N., & Neves, L. (2019). Probabilistic prediction of asphalt pavement performance. *Road Materials and Pavement Design*, 20(sup1), 247–264. <https://doi.org/10.1080/14680629.2019.1593229>
- Bak, I., Overmars, L., & Van der Kruk, T. (2022). *LCA Achtergrondrapport voor Nederlandse branchereferentiemengsels 2022*.
- Bijleveld, F. R., Miller, S. R., & Dorée, A. G. (2015). Making Operational Strategies of Asphalt Teams Explicit to Reduce Process Variability. *Journal of Construction Engineering and Management*, 141(5), 04015002. [https://doi.org/10.1061/\(ASCE\)CO.1943-7862.0000969](https://doi.org/10.1061/(ASCE)CO.1943-7862.0000969)
- Bouman, S., Cuppens, G., Van Dommelen, A., Eijbersen, M., Van Gurp, C., Pouwels, M., Robbemon, P., Roos, H., Sluer, B., Thewessen, B., De Vries, J., & Willemsen, M.-M. (2012). *Achtereendgrondrapport Ontwerpinstrumentarium asfaltverhardingen (OIA)*.
- De Bruyn, S., Ahdour, S., Bijleveld, M., De Graaff, L., Schep, E., Schroten, A., & Vergeer, R. (2017). *Handboek Milieuprijzen*. CE Delft.
- Deb, K. (2001a). *Multi-objective optimization using evolutionary algorithms* (1st ed). John Wiley & Sons.
- Deb, K. (2001b). *Multiobjective Optimization Using Evolutionary Algorithms*. Wiley, New York.
- Deb, K., Pratap, A., Agarwal, S., & Meyarivan, T. (2002). A fast and elitist multiobjective genetic algorithm: NSGA-II. *IEEE Transactions on Evolutionary Computation*, 6(2), 182–197. <https://doi.org/10.1109/4235.996017>
- Dilip, D. M., & Babu, G. L. S. (2021). Reliability-Based Design Optimization of Flexible Pavements Using Kriging Models. *Journal of Transportation Engineering, Part B: Pavements*, 147(3), 1–14. <https://doi.org/10.1061/JPEODX.0000306>
- Ecochain Helix (3.5.57)*. (2022). Ecochain Technologies B.V.
- Espinoza, M., Campos Campos, N., Yang, R., Ozer, H., Aguiar-Moya, J., Baldi Sevilla, A., & Loria Salazar, L. (2019). Carbon Footprint Estimation in Road Construction: La Abundancia–Florenia Case Study. *Sustainability*, 11, 2276. <https://doi.org/10.3390/su11082276>
- Ferreira, A., & Santos, J. (2012). Pavement Design Optimization Considering Costs and Preventive Interventions. *Journal of Transportation Engineering*, 138, 911–923. [https://doi.org/10.1061/\(ASCE\)TE.1943-5436.0000390](https://doi.org/10.1061/(ASCE)TE.1943-5436.0000390)
- Garbarino, E., Rodriguez Quintero, Rocío., Donatello, S., & Wolf, O. (2016). *Revision of green public procurement criteria for road design, construction and maintenance: Procurement practice guidance document*. Publications Office.
- Gaurav, G., Wojtkiewicz, S., & Khazanovich, L. (2011). Optimal design of flexible pavements using a framework of DAKOTA and MEPDG. *International Journal of Pavement Engineering - INT J PAVEMENT ENG*, 12, 137–148. <https://doi.org/10.1080/10298436.2010.535535>
- Hadi, M. N. S., & Arfiadi, Y. (2001). Optimum rigid pavement design by genetic algorithms. *Computers & Structures*, 79(17), 1617–1624. [https://doi.org/10.1016/S0045-7949\(01\)00038-4](https://doi.org/10.1016/S0045-7949(01)00038-4)
- Huang, Y. H. (2004). *Pavement analysis and design* (2nd ed). Pearson/Prentice Hall.
- LaTorre, A., Molina, D., Osaba, E., Del Ser, J., & Herrera, F. (2020). *Fairness in Bio-inspired Optimization Research: A Prescription of Methodological Guidelines for Comparing Meta-heuristics* (arXiv:2004.09969). arXiv. <http://arxiv.org/abs/2004.09969>
- Matlab R2021b* (9.11.0.1769968). (2021). The Mathworks, Inc.
- Miettinen, K. (2008). Introduction to Multiobjective Optimization: Noninteractive Approaches. In J. Branke, K. Deb, K. Miettinen, & R. Słowiński (Eds.), *Multiobjective Optimization: Interactive and Evolutionary Approaches* (pp. 1–26). Springer Berlin Heidelberg. https://doi.org/10.1007/978-3-540-88908-3_1

- Miettinen, K. (2012). *Nonlinear multiobjective optimization* (Vol. 12). Springer Science & Business Media.
- Miller, S., Huerne, H., & Dorée, A. (2010). *Role of action research in dealing with a traditional process* (pp. 92–101).
- Miner, M. A. (1945). Cumulative damage in fatigue. *Journal of Mechanical Engineering*.
- Odemark, N. (1949). *Investigations as to the elastic properties of soils and design of pavements according to the theory of elasticity*.
- Peddinti, P. R. T., Munwar Basha, B., & Saride, S. (2020). System Reliability Framework for Design of Flexible Pavements. *Journal of Transportation Engineering, Part B: Pavements*, 146(3), 04020043. <https://doi.org/10.1061/JPEODX.0000186>
- Pryke, A., Evdorides, H., & Ermaileh, R. A. (2006). Optimization of pavement design using a genetic algorithm. *2006 IEEE International Conference on Evolutionary Computation*, 1095–1098. <https://doi.org/10.1109/CEC.2006.1688431>
- Rajbongshi, P., & Das, A. (2008). Optimal Asphalt Pavement Design Considering Cost and Reliability. *Journal of Transportation Engineering*, 134(6), 255–261. [https://doi.org/10.1061/\(ASCE\)0733-947X\(2008\)134:6\(255\)](https://doi.org/10.1061/(ASCE)0733-947X(2008)134:6(255))
- Reeves, C. R. (2010). Genetic Algorithms. In M. Gendreau & J.-Y. Potvin (Eds.), *Handbook of Metaheuristics* (Vol. 146, pp. 109–139). Springer US. https://doi.org/10.1007/978-1-4419-1665-5_5
- Sahis, M. K., & Biswas, P. P. (2021). Optimization of Bituminous Pavement Thickness using Mechanistic-Empirical Strain-Based Design Approach. *Civil Engineering Journal*, 7(5), 804–815. <https://doi.org/10.28991/cej-2021-03091691>
- Santos, J., Ferreira, A., & Flintsch, G. (2016, July). *An Adaptive Hybrid Genetic Algorithm for Pavement Management*.
- Santos, J., Ferreira, A., Flintsch, G., & Cerezo, V. (2017a). *A multi-objective optimization approach for sustainable pavement management in: Life-Cycle of Engineering Systems: Emphasis on Sustainable Civil Infrastructure* (pp. 365–372).
- Santos, J., Ferreira, A., Flintsch, G., & Cerezo, V. (2017b, June). *Consideration of life cycle greenhouse gas emissions in optimal pavement maintenance programming: A comparison between single- and multi-objective optimization approaches*.
- Santos, J., Ferreira, A., Flintsch, G., & Cerezo, V. (2018). A multi-objective optimisation approach for sustainable pavement management. *Structure and Infrastructure Engineering*, 1–15. <https://doi.org/10.1080/15732479.2018.1436571>
- Saride, S., Peddinti, P. R. T., & Basha, M. B. (2019). Reliability Perspective on Optimum Design of Flexible Pavements for Fatigue and Rutting Performance. *Journal of Transportation Engineering, Part B: Pavements*, 145(2), 04019008. <https://doi.org/10.1061/JPEODX.0000108>
- Schwarz, A., Overmars, L., Bizarro, D. G., Keijzer, E., Kuling, L., & Van Horssen, A. (2020). *LCA Achtergrondrapport voor brancherepresentatieve Nederlandse asfaltmengsels 2020*. TNO.
- Sivanandam, S. N., & Deepa, S. N. (2008). Terminologies and Operators of GA. In *Introduction to Genetic Algorithms* (pp. 39–81). Springer London NetLibrary, Inc. [distributor].
- Skar, A., & Andersen, S. (2020). ALVA: An adaptive MATLAB package for layered viscoelastic analysis. *Journal of Open Source Software*, 5(55), 2548. <https://doi.org/10.21105/joss.02548>
- Specificaties Ontwerp Asfaltverhardingen*. (2016).
- Standaard RAW Bepalingen*. (2020). CROW.
- Strickland, D. (2015). Design of flexible pavements. In R. N. Hunter, A. Self, & J. Read, *The Shell Bitumen Handbook* (6th ed., pp. 347–377). ICE Publishing.
- Talbi, E.-G. (2009). *Metaheuristics: From design to implementation*. John Wiley & Sons.
- Van der Kruk, T., & Overmars, L. (2022). *Product Category Rules voor bitumineuze materialen in verkeersdragers en waterwerken in Nederland ("PCR Asfalt")*.
- Vasudevan, J., Raju, S., & Lu, J. (2015). Properties of asphalts. In R. N. Hunter, A. Self, & J. Read, *The Shell Bitumen Handbook* (6th ed., pp. 479–501). ICE Publishing.

Yu, X., & Gen, M. (2010). *Introduction to Evolutionary Algorithms* (Vol. 0). Springer London.
<https://doi.org/10.1007/978-1-84996-129-5>

Appendix A

Table 9. Dataset considered in the application of the CMOO approach for the flexible pavement design problem

Mixture ID	Production plant	Mixture position	General mixture name	Thickness boundaries (mm)	Thickness step size (mm)	PC	PC _{base}	PC _{bind}	PC _{bind,PA}	$ECI_{A1-3}^{1,3}$	$ECI_{A1-3}^{1,4}$
1	1	Base/bind	AC 22 BASE/BIND	55-90	5	N/A	1-4	1-4	1-3	10	10
2	1	Base/bind	AC 22 BASE/BIND	55-90	5	N/A	1-4	1-4	2-4	8	8
3	1	Bind	AC 16 BIND	40-60	5	N/A	N/A	N/A	2-4	13	13
4	1	Base/bind	AC 16 BASE/BIND	40-60	5	N/A	1-4	1-4	2-4	3	7
5	1	Base/bind	AC 22 BASE/BIND Mod.	55-90	5	N/A	1-4	1-4	2-4	11	11
6	1	Bind	AC 22 BIND Mod.	55-90	5	N/A	N/A	1-4	N/A	12	12
7	1	Bind	AC 16 BIND	40-60	5	N/A	N/A	1-4	2-4	9	9
8	3	Base/bind	AC 16 BASE/BIND	40-60	5	N/A	1-4	2-3	2-4	4	3
9	3	Base/bind	AC 22 BASE/BIND	55-90	5	N/A	1-4	2-3	2-4	4	3
10	3	Base/bind	AC 16 BASE/BIND	40-60	5	N/A	1-4	2-3	2-4	6	5
11	3	Base/bind	AC 22 BASE/BIND	55-90	5	N/A	1-4	2-3	2-4	6	5
12	1	Surface	AC 8 SURF	20-30	5	1-2	N/A	N/A	N/A	19	20
13	1	Surface	AC 11 SURF	30-50	5	2-4	N/A	N/A	N/A	18	18
14	1	Surface	AC 16 SURF	40-60	5	2	N/A	N/A	N/A	16	16
15	1	Surface	AC 16 SURF	40-60	5	2-4	N/A	N/A	N/A	15	15
16	1	Surface	AC 16 SURF	40-60	5	1-3	N/A	N/A	N/A	14	14
17	1	Surface	SMA-NL 8G	20-35	5	1-4	N/A	N/A	N/A	22	22
18	1	Surface	SMA-NL 8G+ Mod.	20-35	5	1-4	N/A	N/A	N/A	28	28
19	1	Surface	SMA-NL 8A	20-35	5	1-4	N/A	N/A	N/A	21	21
20	1	Surface	SMA-NL 8B	20-35	5	1-4	N/A	N/A	N/A	25	25
21	1	Surface	SMA-NL 8B	20-35	5	1-4	N/A	N/A	N/A	26	26
22	1	Surface	SMA-NL 8B Mod.	20-35	5	1-4	N/A	N/A	N/A	32	32
23	1	Surface	SMA-NL 8B	20-35	5	1-4	N/A	N/A	N/A	27	27
24	1	Surface	SMA 11G Mod.	30-40	5	1-4	N/A	N/A	N/A	30	30
25	1	Surface	SMA-NL 11A	30-40	5	1-4	N/A	N/A	N/A	20	19
26	1	Surface	SMA-NL 11B	30-40	5	1-4	N/A	N/A	N/A	23	23
27	1	Surface	SMA-NL 11B	30-40	5	1-4	N/A	N/A	N/A	23	23
28	1	Surface	SMA-NL 11B	30-40	5	1-4	N/A	N/A	N/A	31	31
29	1	Surface	SMA-NL 11B	30-40	5	1-4	N/A	N/A	N/A	29	29
30	1	Surface	SMA-NL 11B	30-40	5	1-4	N/A	N/A	N/A	33	33
31	1	Surface	PA 16	50-60	5	1-4	N/A	N/A	N/A	17	17
32	2	Subbase	Mixed granulate	250-350	50	1-4	N/A	N/A	N/A	1	1
33	2	Subbase	Hydraulic mixed granulate	250-350	50	1-4	N/A	N/A	N/A	2	2

Table 9. (continued)

Mixture ID	$C_{A1-3}^{1,3}$	$C_{A1-3}^{1,4}$	ρ^2	Mixture type ⁵	c_1^{f2}	c_2^{f2}	c_3^{f2}	c_4^{f2}	c_5^{f2}	H_f^2	c_1^{E2}	c_2^{E2}	c_3^{E2}	c_4^{E2}	T^{E2}	f^{E2}	CK^{E2}	E^2	Poisson's ratio
1	9	9	7	7	6	1	1	6	6	1	5	1	1	1	1	1	1	N/A	0.35
2	8	8	6	7	3	1	1	3	2	6	2	1	1	1	1	1	1	N/A	0.35
3	14	14	5	7	2	1	1	2	2	1	3	1	1	1	1	1	1	N/A	0.35
4	7	7	15	7	5	1	1	4	5	1	4	1	1	1	1	1	1	N/A	0.35
5	11	11	1	8	7	1	1	9	9	11	1	1	1	1	1	1	1	N/A	0.35
6	12	12	2	8	1	1	1	1	4	5	6	1	1	1	1	1	1	N/A	0.35
7	10	10	10	7	4	1	1	5	1	4	11	1	1	1	1	1	1	N/A	0.35
8	5	5	2	7	8	1	1	7	7	9	7	1	1	1	1	1	1	N/A	0.35
9	5	5	2	7	8	1	1	7	7	9	7	1	1	1	1	1	1	N/A	0.35
10	3	3	8	7	9	1	1	10	10	6	9	1	1	1	1	1	1	N/A	0.35
11	3	3	8	7	9	1	1	10	10	6	9	1	1	1	1	1	1	N/A	0.35
12	19	19	12	1	N/A	N/A	N/A	N/A	N/A	N/A	15	1	1	1	1	1	1	N/A	0.35
13	17	17	15	1	N/A	N/A	N/A	N/A	N/A	N/A	12	1	1	1	1	1	1	N/A	0.35
14	16	16	14	1	N/A	N/A	N/A	N/A	N/A	N/A	12	1	1	1	1	1	1	N/A	0.35
15	15	15	11	2	N/A	N/A	N/A	N/A	N/A	N/A	12	1	1	1	1	1	1	N/A	0.35
16	13	13	12	2	N/A	N/A	N/A	N/A	N/A	N/A	15	1	1	1	1	1	1	N/A	0.35
17	23	23	29	15	N/A	N/A	N/A	N/A	N/A	N/A	17	N/A	N/A	N/A	N/A	N/A	N/A	N/A	0.35
18	31	31	30	18	N/A	N/A	N/A	N/A	N/A	N/A	17	N/A	N/A	N/A	N/A	N/A	N/A	N/A	0.35
19	24	24	18	15	N/A	N/A	N/A	N/A	N/A	N/A	17	N/A	N/A	N/A	N/A	N/A	N/A	N/A	0.35
20	25	25	20	15	N/A	N/A	N/A	N/A	N/A	N/A	17	N/A	N/A	N/A	N/A	N/A	N/A	N/A	0.35
21	25	25	25	15	N/A	N/A	N/A	N/A	N/A	N/A	17	N/A	N/A	N/A	N/A	N/A	N/A	N/A	0.35
22	29	29	23	16	N/A	N/A	N/A	N/A	N/A	N/A	17	N/A	N/A	N/A	N/A	N/A	N/A	N/A	0.35
23	27	27	25	15	N/A	N/A	N/A	N/A	N/A	N/A	17	N/A	N/A	N/A	N/A	N/A	N/A	N/A	0.35
24	33	33	29	16	N/A	N/A	N/A	N/A	N/A	N/A	17	N/A	N/A	N/A	N/A	N/A	N/A	N/A	0.35
25	22	22	15	15	N/A	N/A	N/A	N/A	N/A	N/A	17	N/A	N/A	N/A	N/A	N/A	N/A	N/A	0.35
26	20	20	19	15	N/A	N/A	N/A	N/A	N/A	N/A	17	N/A	N/A	N/A	N/A	N/A	N/A	N/A	0.35
27	20	20	23	15	N/A	N/A	N/A	N/A	N/A	N/A	17	N/A	N/A	N/A	N/A	N/A	N/A	N/A	0.35
28	30	30	27	16	N/A	N/A	N/A	N/A	N/A	N/A	17	N/A	N/A	N/A	N/A	N/A	N/A	N/A	0.35
29	28	28	20	16	N/A	N/A	N/A	N/A	N/A	N/A	17	N/A	N/A	N/A	N/A	N/A	N/A	N/A	0.35
30	32	32	22	16	N/A	N/A	N/A	N/A	N/A	N/A	17	N/A	N/A	N/A	N/A	N/A	N/A	N/A	0.35
31	18	18	31	10	N/A	N/A	N/A	N/A	N/A	N/A	31	N/A	N/A	N/A	N/A	N/A	N/A	N/A	0.35
32	1	1	33	N/A	N/A	N/A	N/A	N/A	N/A	N/A	N/A	N/A	N/A	N/A	N/A	N/A	N/A	2	0.35
33	2	2	32	N/A	N/A	N/A	N/A	N/A	N/A	N/A	N/A	N/A	N/A	N/A	N/A	N/A	N/A	1	0.35

¹ Ascending ranking order meaning from lowest to highest value.² Descending ranking order meaning from highest to lowest value.³ Cost and ECI values for case studies 1-4.⁴ Cost and ECI values for case study 5.⁵ Mixture type based on Bak et al. (2022) for the cost and ECI calculations of LCA stage A5.